ISSN 1063-7710, Acoustical Physics, 2015, Vol. 61, No. 5, pp. 547–555. © Pleiades Publishing, Ltd., 2015.
Original Russian Text © A.A. Lunkov, 2015, published in Akusticheskii Zhurnal, 2015, Vol. 61, No. 5, pp. 596–604.

OCEAN ACOUSTICS.
HYDROACOUSTICS

Interference Structure of Low-Frequency Reverberation Signals in Shallow Water

A. A. Lunkov

Wave Research Center, Prokhorov General Physics Institute, Russian Academy of Sciences, ul. Vavilova 38, Moscow, 119991 Russia

e-mail: landr2004@mail.ru

Received December 22, 2014

Abstract—Using numerical simulation, an analysis was conducted of the interference structure of a bottom-scattered sound field generated by a wideband point source in shallow water under winter and summer conditions. The scattered signals were received from the place where the source was located and were subjected to Fourier transform with a sliding window. The paper demonstrates the possibility of estimating the waveguide invariant for backscattered signals when processing the sound intensity distributions in wide frequency and distance ranges up to the scattering area. A technique is proposed for reconstructing the two-dimensional field of internal waves using variations of the interference pattern of reverberation signals. The influence of wind surface waves on the degree of interference band contrast is illustrated.

Keywords: shallow-water acoustics, reverberation, waveguide invariant, wind waves, internal waves

DOI: 10.1134/S1063771015040065

1. INTRODUCTION

For long-range remote sounding of shallow-water areas typical of an ocean shelf, it is convenient to use low-frequency (up to several hundred hertz) acoustic waves, since only they can propagate underwater to large distances. Usually to monitor the spatiotemporal variability of large water areas, substantial facilities are required, namely, the use of a set of spatially diverse receiving and transmitting elements like those in classic tomography schemes [1]. The results of recent investigations in the field of passive tomography give hope for simplifying the implementation of tomographic schemes [2], but here the critical moment is the signal accumulation time, which can exceed the characteristic stability time of the marine environment. Therefore, it is an important task to develop physical fundamentals for a more operative, but at the same time no less informative method of remote sounding. The basic idea of the method proposed in this paper is an analysis of the interference pattern of backscattered signals arriving from different distances and directions relative to a point sound source. Note that for the majority of conditions, except for the case of a near-surface sound channel, reverberation is conditioned by sound scattering on bottom irregularities. At low frequencies (up to 500 Hz) and for a mild wind, the bottom backscattering coefficient, as a rule, is 10–30 dB higher than the similar value for the water surface [3]. The theoretical and experimental research on estimating this coefficient is reviewed in [4].

Now, the majority of research in underwater acoustics is concentrated on shallow-water regions [3] (shelf zones, large lakes, water reservoirs, etc.), which play a very important role in ensuring human vital activity. Internal waves represent one of the most significant hydrodynamic processes in such water areas in summer, when there is a pronounced density stratification with depth (pycnocline). They play a key role in mixing of water layers and transfer of biomass and runoff, thus influencing climate and the ecological situation in near-coastal zones. Their monitoring is undoubtedly an important task. In addition to conventional point measurements of internal wave parameters using chains of thermistors, remote acoustic methods, including those based on recording backscattered signals, can aid in determining the averaged spatial characteristics of internal waves at large distances.

Works [5, 6] are well known, which in deep-ocean field experiments demonstrated the possibilities of applying signals backscattered from the bottom relief and marine fauna to visualize the migration of large schools of fish at distances of several tens of kilometers from the source–receiver system. In [7], similar signals are used to remotely estimate bottom irregularities in the near-coastal zone in an area of up to 10^4 km^2.

In the above-mentioned works, the authors, in analyzing reverberation signals, limited themselves to considering their mean intensity [5–7]; however, recently, there has been greater focus on the coherent properties of such signals [8–12]. As was shown in [11, 12], in the bottom reverberation distribution when

depicted on the "arrival time—frequency" plane, the interference pattern of the sound field manifests itself similarly to what takes place for the intensity of a direct signal in "distance–frequency" coordinates and which can be described by the waveguide invariant introduced by S.D. Chuprov [13]. In addition, the presence of hydrodynamic irregularities leads to variation of the interference pattern of the sound field with time, namely, to its shift in frequency [14], which in turn can be used to monitor these inhomogeneities.

In the general case, variations in the interference pattern of the scattered field will depend on the direction from which the signal is received. The possibility of selecting reverberation signals arriving from various directions owing to the formation of the directivity pattern in the horizontal plane was demonstrated in a field experiment [7, 11]. However, the use of a linear scalar receiving array led to ambiguity of starboard and port.[1] A way out of this complicated situation may be to apply vector scalar arrays [15] that record, in addition to acoustic pressure, two horizontal components of the particle velocity. In this case, the mirror lobe in the directivity pattern might be suppressed to a significant degree. Note that a rigorous mathematical description of the algorithm that isolates reverberation signals arriving from different directions using vector scalar arrays goes beyond the scope of this paper; the author limits himself to considering only sound pressure fields.

When choosing the length of the receiving array, it is necessary to take into account the transverse radius of the sound field coherency. As W. Kerry [16] and J. Lynch's [17] experimental works have shown, in shallow water this radius on average is 30 λ (λ is the wavelength of the sound wave) and weakly depends on the distance to the source.

The aim of this paper is to study, using numerical experiments, the features of the interference pattern of a bottom-scattered sound field formed along a given direction in summer and winter conditions in the presence of hydrodynamic inhomogeneities, as well as to estimate the possibility of reconstructing the internal wave parameters from variations in this pattern.

2. MODE DESCRIPTION OF BACKSCATTERED SIGNALS

As an acoustic model of shallow water, let us consider a waveguide of constant depth H. Let us introduce a cylindrical coordinate system (r, φ, z), the origin of which is located on the upper boundary of the waveguide and the z axis is directed vertically downward. The sound speed $c(r, \varphi, z)$ in the general case depends on all three variables. The sound source is on the z axis at depth z_s and emits a signal in the frequency band from f_1 to f_2. The center of the horizontal array used to isolate scattered signals arriving from different directions is on the same axis at depth z_r. The length of the array is chosen equal to 10 λ (λ is the wavelength corresponding to the mean emitted frequency), which is significantly less that the mean transverse radius of the sound field coherency: 30 λ. The angular resolution of the array, if the estimate for the free space is used, is $\delta\varphi \sim \lambda/L \approx 6^\circ$, and the far field approximation is valid for distances of $r_{\text{far}} > 2L^2/\lambda = 200\,\lambda$ (for a frequency of 200 Hz, $r_{\text{far}} > 1500$ m). We will consider that the waveguide characteristics in the range of angles $\delta\varphi$ weakly depends on φ.

Without loss of generality, we fix a certain direction φ_0 from which we isolate a reverberation signal and pass to solving the two-dimensional problem in (r, z), coordinates using the uncoupled azimuth approximation $(N \times 2D)$, as was done in [11]. The transfer function of an inhomogeneous waveguide between the sound source moored at depth z_s and the elemental scattering area located at distance r ($r \gg \lambda$) in direction φ_0 can be represented as the sum of normal waves (modes) [3]:

$$Z(\omega, r; z_s) = \sum_{m=1}^{M(\omega)} C_m(\omega, r; z_s)\psi_m(\omega, r, H) \times \frac{\exp\left(i\int_0^r q_m(\omega, r')dr'\right)}{\sqrt{\int_0^r q_m(\omega, r')dr'}} = \sum_{m=1}^{M(\omega)} A_m(\omega, r, H; z_s)\exp\left(i\int_0^r q_m(\omega, r')dr'\right). \quad (1)$$

Here, $\omega = 2\pi f$ is the circular frequency, ψ_m and $\xi_m = q_m + i\gamma_m/2$ are the eigenfunctions (waveguide modes) and eigenvalues (propagation constants) of the Sturm–Liouville problem, and $M(\omega)$ is the overall number of energy-carrying modes at frequency ω. The modal excitation coefficients C_m are determined from the solution to the following system of differential equations (the dependence on frequency ω is omitted for brevity):

$$\frac{dC_m(r')}{dr'} = -\frac{\gamma_m}{2}C_m(r') + i\sum_{n=1}^{M}\nu_{nm}(r')C_n(r') \times \exp\left(i\int_0^{r'}\left(q_n(r'') - q_m(r'')\right)dr''\right), \quad m = \overline{1, M}$$

with the initial conditions $C_m(0) = \psi_m(z_s)$, ν_{nm} are the mode coupling coefficients.

[1] Generally speaking, instead of directional reception, directional emission can be used.

When calculating the transfer function of the waveguide with surface waves, decomposition (1) is usually done for the modes of an unperturbed waveguide, i.e., $\psi_m(r,z) = \psi_m^0(z)$ and $\int_0^r q_m(r')dr' = q_m^0 r$, and the mode coupling coefficients have the form

$$\nu_{nm}(r') = \zeta_{sw}(r')\frac{1}{2\sqrt{q_m^0 q_n^0}}\frac{\partial\psi_m^0}{\partial z}\bigg|_{z=0}\frac{\partial\psi_n^0}{\partial z}\bigg|_{z=0},$$

where $\zeta_{sw}(r')$ is the vertical displacement of the free boundary with respect to the position of equilibrium at a point at distance r'.

Calculations in the presence of background internal waves can be performed in the adiabatic approximation, which assumes that $\nu_{nm} = 0$ and $C_m(r;z_s) = \psi_m(0;z_s)$.

The complex amplitude of a sound signal that passed from the source to the scattering area and back, can be approximately written as follows for a monostatic scheme of recording reverberation and assuming isotropic scattering in the vertical plane:

$$P_{sc}(\omega,r) = U(\omega)Z(\omega,r;z_s)Z(\omega,r;z_r) \approx U(\omega)\sum_{m=1}^{M(\omega)}\sum_{m'=1}^{M(\omega)} B_{mm'}(\omega,r,H;z_s,z_r) \times \exp\left(i\int_0^r \left(q_m(\omega,r') + q_{m'}(\omega,r')\right)dr'\right). \quad (2)$$

Here, $U(\omega)$ is the spectrum of the emitted signal, $B_{mm'}(\omega,r,\ H;z_s,z_r) = \eta(r)A_m(\omega,r,\ H;z_s)F_{mm'}A_{m'}(\omega,r,H;z_r)$, z_r is the depth of the receiving element, $\eta(r) = \sigma(r)\exp(i\vartheta(r))$ is a random function characterizing fluctuations in the scattering field [10, 11]; amplitude $\sigma(r)$ and phase $\vartheta(r)$ are statistically independent quantities, the first of which is Rayleigh-distributed and the second is uniformly distributed; $F_{mm'} = \sqrt{\sin\theta_m \sin\theta_{m'}}$ is the Lambert law, which describes rescattering from mode m to mode m', where $\theta_m = \arccos(q_m/k(H))$ is the grazing angle of a Brillouin ray corresponding to the mth mode, and $k(H) = \omega/c(H)$ is the wavenumber near the bottom.

Integrating expression (2) over all scattering areas located at different distances r and performing Fourier transform, we obtain the time realization of the reverberation signal:

$$p_{sc}(t) = \int_0^{\infty}\int_{-\infty}^{+\infty} P_{sc}(\omega,r)\exp(-i\omega t)d\omega dr = \int_0^{\infty}\int_{-\infty}^{+\infty} U(\omega)\sum_{m=1}^{M(\omega)}\sum_{m'=1}^{M(\omega)} B_{mm'}(\omega,r) \times \exp\left(i\int_0^r \left(q_m(\omega,r') + q_{m'}(\omega,r')\right)dr' - i\omega t\right)d\omega dr. \quad (3)$$

If a complex signal is emitted (e.g., M-sequence, LFM, etc.), then it is expedient to perform correlation processing at the receiver:

$$y_{sc}(\tau) = \int_{-\infty}^{+\infty} p_{sc}(t)s(t-\tau)dt. \quad (4)$$

To obtain the frequency–time dependences of the amplitude of the received signal (spectrograms), short-time Fourier transform is applied.

$$S_{sc}(\omega,t) = \left|\int_{-\infty}^{+\infty} y_{sc}(\tau)W(\tau - t)\exp(i\omega\tau)d\tau\right|, \quad (5)$$

where the Hemming window is used as the weight function $W(\tau - t)$ [18]:

$$W(\tau - t) = \begin{cases} 0.54 + 0.46\cos\left(\dfrac{2\pi(\tau - t)}{T_w}\right), & |\tau - t| \le T_w/2, \\ 0, & |\tau - t| > T_w/2, \end{cases}$$

where T_w is the window width. It is important to note that precisely in the dependences $S_{sc}(\omega,t)$, a two-dimensional interference structure of the scattered sound field manifests itself.

3. MODEL WAVEGUIDE PARAMETERS

Sound propagation and scattering are numerically simulated using formulas (1)–(5) for a waveguide with constant depth $H = 80$ m in the frozen medium approximation. The bottom is a fluid absorbing half-space, primarily homogeneous, with the following parameters: sound speed $c_b = 1800$ m/s, density $\rho_b = 1800$ kg/m^3, imaginary part of the refractive index $\alpha_b = 0.012$. Backscattering of sound signals is conditioned by the presence of small bottom roughnesses and weak inhomogeneities under its surface. The correlation radius of these perturbations is significantly less than the period of interference beats of the sound field.

Figure 1 shows the vertical sound speed profiles $c(z)$ in the water in summer and winter conditions. For the summer, the mean unperturbed profile and profiles corresponding to different shifts in the thermocline ζ_{iw} in the internal wave field are shown.

A nondirectional single sound source is located 5 m from the bottom at a depth of $z_s = 75$ m and emits an LFM signal in the frequency band of $f = 100$–300 Hz with a duration of 1 s. The receiver system that isolates signals from different directions is moored at the same depth as the source, i.e., $z_r = z_s$. The studied range of distances from which bottom-scattered signals are received is $r = 2$–12 km (far field). Thus, the duration of the analyzed reverberation signal is around 15 s.

The stochastic dependence $\eta(r)$, describing fluctuations of the scattering field (see commentary to formula (2)) is simulated with a step of $\Delta r = 25$ m. Because we are interested only in relative variations in

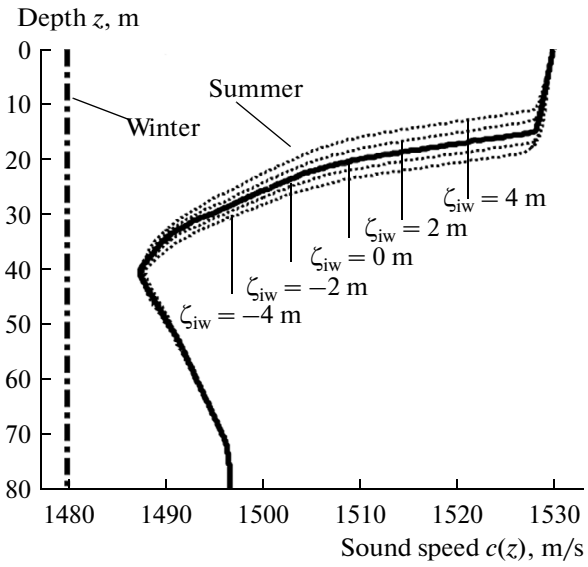

Fig. 1. Vertical sound speed profile in winter and summer conditions.

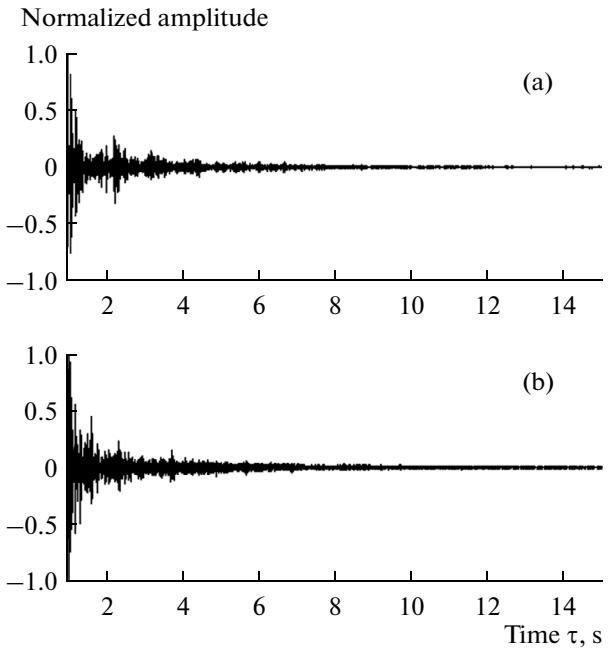

Fig. 2. Time realizations of reverberation signal at output of correlation receiver in unperturbed waveguide: (a) summer, (b) winter.

the interference structure of the bottom-scattered sound field and the problem is solved in the absence of noise, the mean amplitude $\overline{\sigma}$ for this dependence is chosen equal to unity for simplicity. (When it is necessary to calculate the absolute values of the amplitude of the scattered field, one should use the relationship between quantity $\overline{\sigma}$ and the averaged backscattering coefficient [10], which is determined experimentally.)

Random realizations of surface waves $\zeta_{sw}(r')$ are calculated with the empirical Pierson–Neumann spectrum [19] for a wind speed of $V_{\text{wind}} = 12$ m/s and the directivity characteristic $\cos^2\varphi$. It is assumed that surface waves propagate along the direction φ_0 from which reverberation signals are recorded.

When analyzing variations in the parameters of the scattered sound field related to hydrodynamic variability in the waveguide column, two simplified internal wave models are used. The first is long-period (tidal) waves, which lead to identical, over the entire observation region, vertical shifts in the thermocline ζ_{iw}. The second model represents quasi-monochromatic internal waves with a period of $\lambda_{\text{iw}} = 10$ km and a narrow directivity characteristic, which propagate in the same direction φ_0 as surface waves. In the first case, the waveguide remains horizontally uniform, and in the second, vertical shifts of the thermocline depend on distance:

$$\zeta_{\text{iw}}(r') = A_{\text{iw}} \sin(k_{\text{iw}} r' + \phi), \qquad (6)$$

where $k_{\text{iw}} = 2\pi/\lambda_{\text{iw}}$ is the wavenumber of the internal wave. The amplitude of internal waves is chosen equal to $A_{\text{iw}} = 4$ m, which is a value typical of a shelf zone of the World Ocean in the summer [14]. In the field of internal waves, the first gravitational mode dominates.

4. REVERBERATION IN A HORIZONTALLY UNIFORM WAVEGUIDE

Time realizations of a bottom-scattered signal that passed through correlation filter (4) are shown in Fig. 2 for an unperturbed horizontally uniform waveguide in winter and summer conditions. Figure 3 shows the spectrograms corresponding to these realizations. To calculate the spectrograms, Fourier transform (5) with a Hemming window with a width of $T_w = 0.2$ s was used. During construction, they were normalized to the maximum value and converted to the decibel scale: $I_{\text{sc}} = 20\lg\dfrac{S_{sc}(\omega,t)}{\max\limits_{\omega,t}(S_{sc}(\omega,t))}$. As one can see, a quite explicit interference structure of the scattered sound field is manifested, but it is more smeared than when direct signals are analyzed. We also note than in winter conditions, when the sound speed is constant over depth, straight interference bands are observed (Fig. 3b), whereas in summer conditions, when the sound speed profile has a negative gradient, these bands are curved (Fig. 3a).

Variability in the interference pattern in the waveguide as a function of distance and frequency can be characterized by scalar parameter β—the waveguide invariant.

Estimating the Waveguide Invariant

In order to use the idea of the waveguide invariant to describe the bottom-scattered sound field in the obtained frequency–time dependences, we switch from time scale t to distance scale r using the relation $r = c_{\text{eff}}t/2$, where c_{eff} is the effective mean sound speed in the waveguide (taken equal to 1500 m/s):

$$S_{\text{sc}}(t,\omega) \to S_{\text{sc}}(r,\omega).$$

The waveguide invariant is commonly estimated using direct signals for small frequency ranges, when the interference bands can be approximated by straight lines [13, 20]. However, the interference pattern of the scattered sound field is quite strongly smeared (see Fig. 3); therefore, to estimate β in such a situation, accumulation and processing of the initial data is needed in wide ranges of r and ω, and the aforementioned approximation ceases to be valid.

As shown in [21], the coordinates of the interference bands on the distance–frequency plane satisfy the differential equation

$$\frac{d\omega}{\omega} = \beta\frac{dr}{r}.$$

Its solution is

$$r = r_1\left(\frac{\omega}{\omega_1}\right)^{\frac{1}{\beta}}, \qquad (7)$$

where $r_1 = r(\omega_1)$. Note that in formula (7), the straight line equation is obtained only in the case of $\beta = 1$.

It is proposed to estimate the waveguide invariant in the case of reverberation signals using an algorithm similar to that proposed in [22] for acoustic noise fields. The first step of the algorithm normalizes the spatial–frequency dependences of the scattered field amplitude:

$$S_{\text{norm}}(r,\omega) = \frac{S_{\text{sc}}(r,\omega)}{\bar{S}_\omega(r)} - 1.$$

Here, $\bar{S}_\omega(r) = \dfrac{1}{\omega_2 - \omega_1}\displaystyle\int_{\omega_1}^{\omega_2} S_{\text{sc}}(r,\omega)d\omega$ is the mean, in terms of frequency, value of the scattered field amplitude at distance r. The second step determines the mean values of quantity $S_{\text{norm}}(r,\omega)$ along the curves described by expression (9) for different β and different initial r_1:

$$\Phi(\beta) = \frac{1}{(r_e - r_i)}\int_{r_i}^{r_e}\frac{1}{L(r_1,\beta)}\left|\int_L S_{\text{norm}}(r,\omega)dl\right|dr_1 = \frac{1}{(r_e - r_i)} \times \int_{r_i}^{r_e}\frac{1}{L(r_1,\beta)}\left|\int_{\omega_1}^{\omega_2} S_{\text{norm}}(r(\omega),\omega)\sqrt{1 + \left(\frac{1}{\beta}\frac{r_1}{\omega}\right)^2\left(\frac{\omega}{\omega_1}\right)^{\frac{2}{\beta}}}d\omega\right|dr_1, \qquad (8)$$

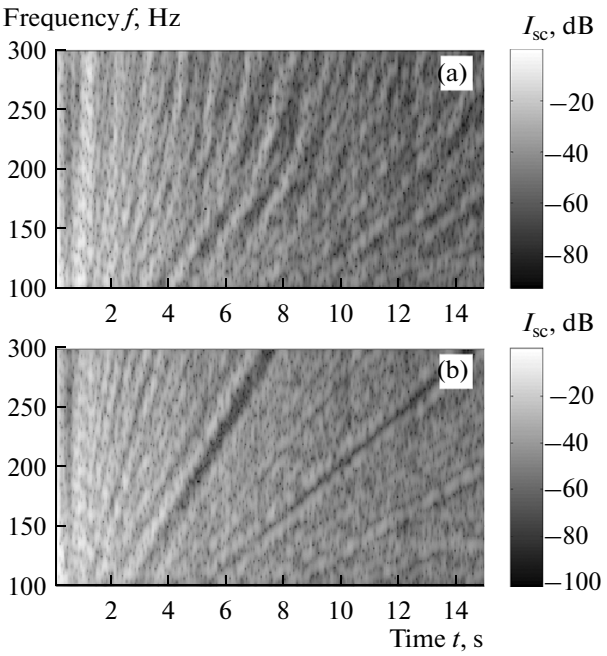

Fig. 3. Spectrograms of reverberation signals shown in Fig. 2.

where $L(r_1,\beta) = \displaystyle\int_{\omega_1}^{\omega_2}\sqrt{1 + \left(\frac{1}{\beta}\frac{r_1}{\omega}\right)^2\left(\frac{\omega}{\omega_1}\right)^{\frac{2}{\beta}}}d\omega$ is the length of the curve and $r_i \ldots r_e$ is the distance range for which the analysis is carried out. The maximum of the distribution $\Phi(\beta)$ corresponds to a certain effective value of waveguide invariant β.

Figure 4 shows the distributions $\Phi(\beta)$ calculated for different conditions. The results shown in Fig. 4a correspond to the spectrograms in Fig. 3. One can see that for a waveguide with a constant sound speed, the maximum of the distribution corresponds, as should have been expected, to $\beta \approx 1$. In summer conditions, the maximum is observed for the largest β values, which is related to the change in the dispersion characteristics of the waveguide modes [23]. Figure 4b shows the variations in distribution $\Phi(\beta)$ as a function of the vertical shift in the thermocline ζ_{iw}. For example, for $\zeta_{\text{iw}} = 4$ m, the position of the maximum shifts by 20% with respect to the unperturbed value corresponding to $\zeta_{\text{iw}} = 0$. Thus, knowing the value of the waveguide invariant and the approximate internal wave model, we can draw a conclusion on the mean, in terms of the waveguide, depth of the thermocline.

It should be noted that additional numerical simulation has shown identical values of the waveguide invariant obtained for direct sound signals and backscattered signals.

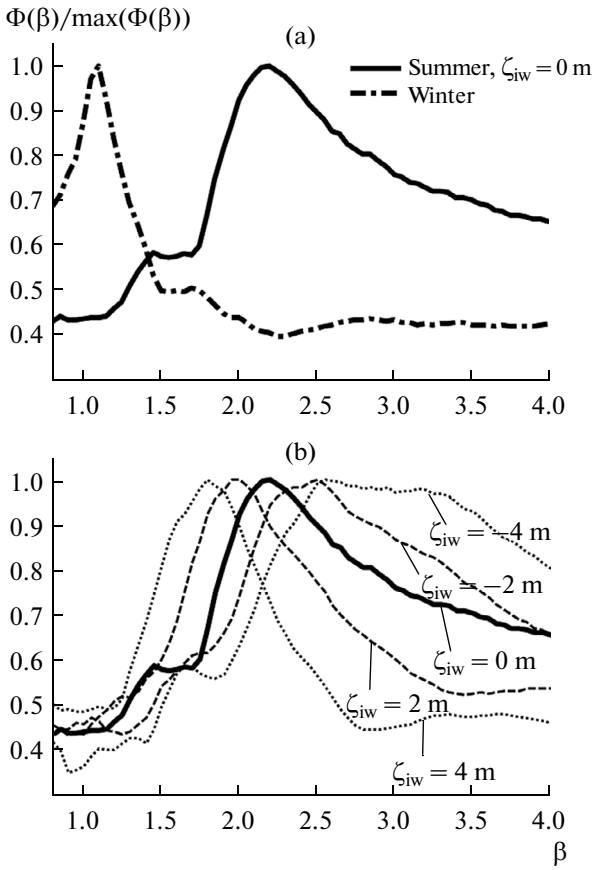

Fig. 4. Normalized distributions Φ(β) for winter and summer conditions (a) and for different values of rise in height of thermocline (b).

5. REVERBERATION IN A HORIZONTALLY NONUNIFORM WAVEGUIDE

It is of interest to estimate the stability of the interference structure of the scattered sound field in the presence of such hydrodynamic inhomogeneities as wind surface waves and background internal waves. A sound field under wind wave conditions is calculated taking into account mode coupling, and under internal wave conditions, the adiabatic approximation is used.

5.1. Surface Waves

Figure 5 shows the spectrograms of reverberation signals in a waveguide with surface waves for a wind speed of 12 m/s for summer and winter conditions. The corresponding mean square value of the wave amplitude is 1.2 m. From a comparison of the results obtained for winter conditions (Figs. 3b, 5b), it follows that surface waves in this period "wash out" interference—the more strongly, the larger the distance and sound frequency. Comparing Figs. 3a and 5a, we arrive at the conclusion that in the summer, surface waves do not affect the contrast of the interference pattern. This is a result of the sound field being screened from a

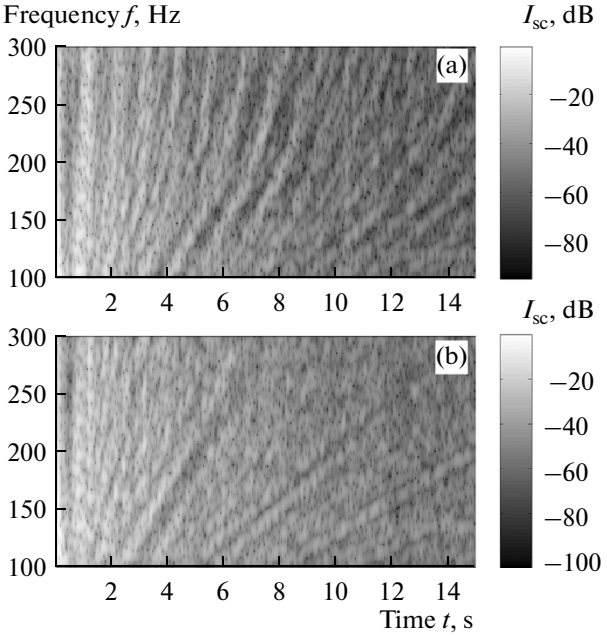

Fig. 5. Same as in Fig. 3 but under wind wave conditions.

rough surface by a warm near-surface layer with a large sound speed. These results correspond to the data obtained in [24] for direct signals. Let us recall that the main source of unstable sound field characteristics in summer conditions is internal waves.

5.2. Internal Waves

Let us consider the features of the formed interference pattern of a scattered sound field during the pass-

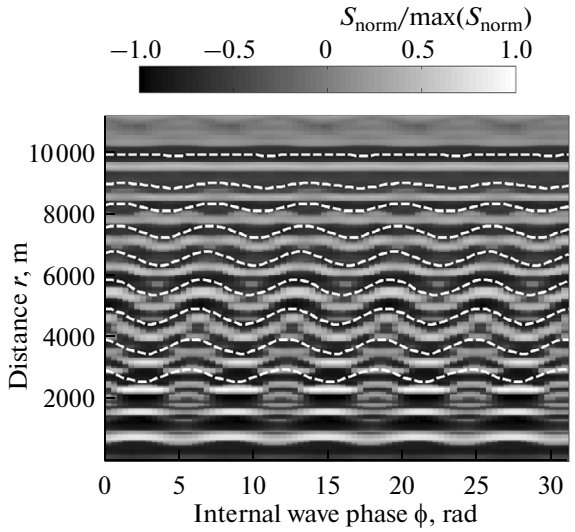

Fig. 6. Variations in spatial interference pattern of scattered sound field at frequency of 200 Hz in presence of internal waves. White dashed lines, estimates of shifts using expression (9).

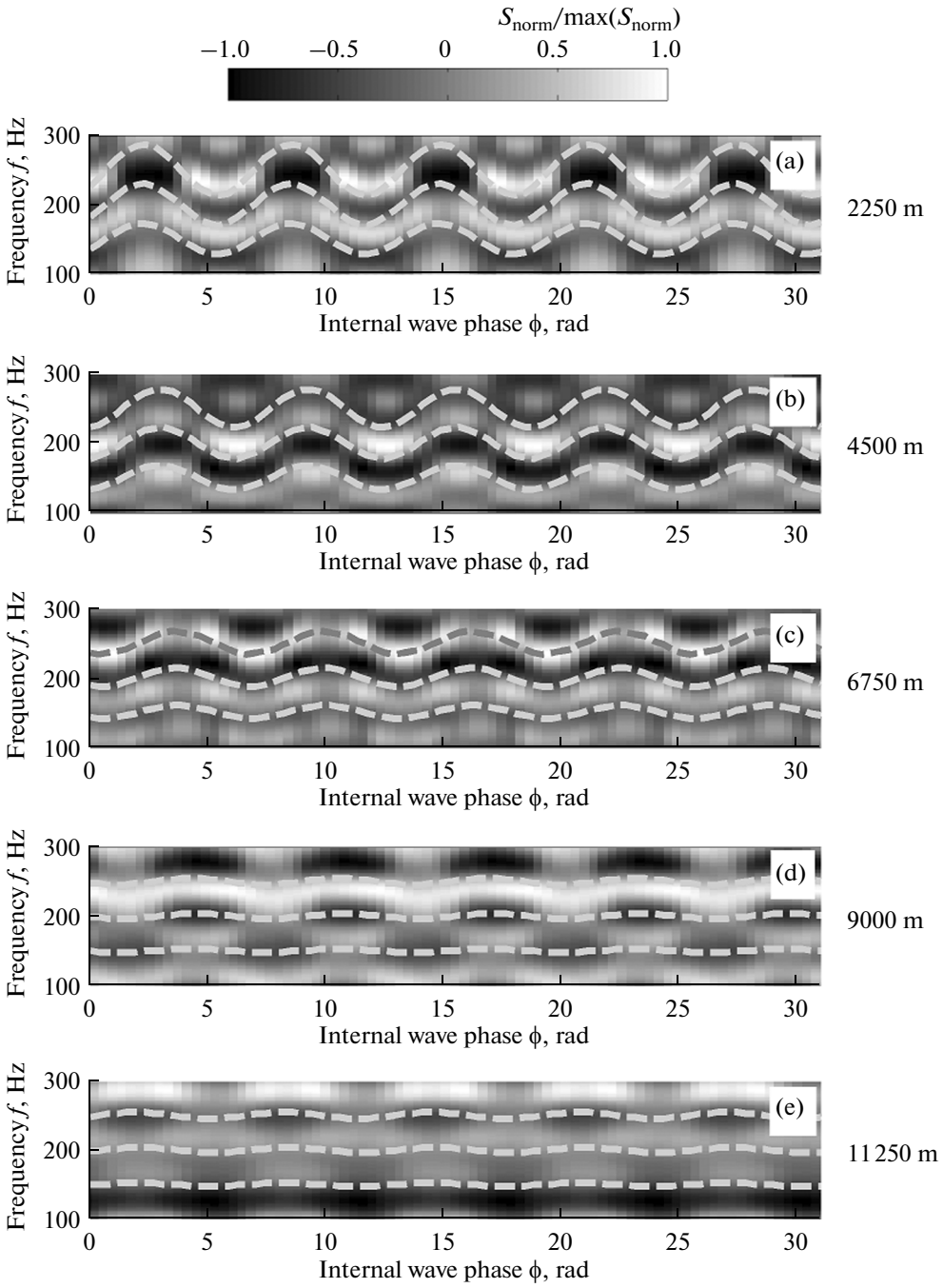

Fig. 7. Variation in interference pattern of scattered sound field in frequency range at different distances r_0 in presence of internal waves. Gray dashed lines, estimates of shifts using expression (10).

ing of an internal wave described by expression (6). For visual illustration, we suppose that the wave phase ϕ constantly changes from 0 to 10π. First, we fix a certain frequency $\omega_0 = 2\pi f_0$ and track variations in the interference structure $S_{sc}(r, \omega_0)$ as a function of ϕ. Figure 6 shows the calculation results for a frequency of 200 Hz. One can see that beginning with a distance of ≈3 km, distinct shifts in the interference maxima occur over distance; however, at a distance equal to the wavelength of the internal wave (10 km), displacements are absent, which is a result of the zero average perturbation along the track. Analysis shows that the size of the shift Δr is well described by the relation

$$\frac{\Delta r}{r} = \alpha \overline{\zeta}_{iw}(r), \qquad (9)$$

where α is some constant determined analytically or by numerical simulation, $\overline{\zeta}_{iw}(r)$ is the mean vertical shift in the thermocline on an acoustic track of length

r (between the source and the scattering area), which in our case is equal to

$$\overline{\zeta}_{\text{iw}}(r) = \frac{1}{r}\int_0^r \zeta(r')dr' = \frac{2A_{\text{iw}}}{k_{\text{iw}}r}\sin\left(\frac{k_{\text{iw}}r}{2}\right)\sin\left(\frac{k_{\text{iw}}r}{2}+\phi\right).$$

Dependences Δr calculated with (9) for different distances r are designated by white dashed lines in Fig. 6. Note that in this work, constant α was determined one time from the condition of best possible fit between the simulation results and the data of estimates (9): 0.02 m^{-1}.

We now fix a certain distance and analyze the frequency shifts of the interference structure of the scattered sound field. Substituting relation (9) into the expression [13]

$$\frac{\Delta\omega}{\omega} = \beta\frac{\Delta r}{r}$$

we obtain the formula for estimating shifts in the interference pattern in the frequency region

$$\frac{\Delta\omega}{\omega} = \alpha\beta\overline{\zeta}_{\text{iw}}(r), \qquad (10)$$

where β is the value of the waveguide invariant for an unperturbed waveguide, in our case equal to 2.2. Figure 7 shows the dependences $S_{\text{sc}}(r_0,\omega)$ for the set of distances r_0. The results of estimating $\Delta\omega$ using expression (10) are shown in the same figure by gray dashed lines. As one can see, the observed frequency shifts in the interference pattern and their estimates virtually coincide. The amplitude of the frequency shift significantly depends on distance.

The good agreement between the data of model experiments and the data of estimates using formulas (9) and (10) is evidence of the fundamental possibility of using shifts in the interference pattern of the scattered sound field to reconstruct the dependence of the mean shift in the thermocline $\overline{\zeta}_{\text{iw}}$ on distance r. In turn, the dependence on the current shift ζ_{iw} on distance r can be calculated using the following relation:

$$\zeta_{\text{iw}}(r) = \overline{\zeta}_{\text{iw}}(r) + r\frac{d\overline{\zeta}_{\text{iw}}}{dr}. \qquad (11)$$

Isolation of reverberation signals arriving from different directions when using a vector-scalar array should make it possible to determine the two-dimensional pattern of the internal wave field $\zeta_{\text{iw}}(r,\varphi)$. To solve similar problems, directional emission can be used.

Finally, let us present the model algorithm for reconstructing the two-dimensional field of vertical shifts in the thermocline $\zeta_{\text{iw}}(r,\varphi)$ according to variations in the interference structure of reverberation signals in a waveguide of constant depth:

(1) obtaining of the interference pattern of the scattered sound field in time (distance)–frequency coordinates for an unperturbed waveguide ($\zeta_{\text{iw}}(r,\varphi)\equiv 0$) using numerical simulation or long-term data observation data under real conditions (the internal wave field is assumed statically homogeneous);

(2) determination of the value of waveguide invariant β and estimation of coefficient α (see expression (9) and subsequent commentary);

(3) recording of the interference pattern of the reverberation signal isolated from some direction φ under internal wave conditions and its comparison with the analogous pattern obtained at the first step for an unperturbed waveguide: determination of shifts $\Delta\omega$ of one pattern with respect to another in the frequency range for different distances r to the scattering area;

(4) calculation of the dependence $\overline{\zeta}_{\text{iw}}(r)$, using expression (10) and estimation of the size of the vertical shift in the thermocline $\zeta_{\text{iw}}(r)$ at different distances r using (11);

(5) repetition of steps 3 and 4 for other reception directions φ.

6. CONCLUSIONS

The numerical simulation results have shown that the interference pattern of a sound field in shallow water manifests itself in backscattered signals both in winter and summer conditions, but it is not very distinct and its observation requires working in wide frequency and distance ranges. The shape of the bend in the observed interference bands has made it possible to estimate the averaged value of the waveguide invariant. Calculations also demonstrated the sensitivity of the mentioned pattern to wind waves in winter and the presence of internal waves in summer. It was discovered that variations in the mean shift of the thermocline in the internal wave field correlates well with shifts in the interference structure in the frequency and spatial ranges, which can be used to monitor these waves.

In subsequent works, the author plans to more rigorously substantiate the possibility of isolating the interference structure of a reverberation signal in a given direction using vector-scalar arrays, as well as to evaluate the accuracy in reconstructing the internal wave field from variations in the interference pattern under different conditions, including in the presence of background noise.

ACKNOWLEDGMENTS

The work was carried out with the financial support of the Russian Foundation for Basic Research, project nos. 14-02-31234 and 13-02-00932.

REFERENCES

1. W. H. Munk, P. Worcester, and C. Wunsch, *Ocean Acoustic Tomography* (University Press, Cambridge, 1995).

2. V. A. Burov, A. V. Grinyuk, V. N. Kravchenko, P. Yu. Mukhanov, S. N. Sergeev, and A. S. Shurup, Acoust. Phys. **60**, 647 (2014).
3. B. G. Katsnelson, V. G. Petnikov, and J. F. Lynch, *Fundamentals of Shallow Water Acoustics* (Springer–Verlag, 2011).
4. A. V. Bunchuk and Yu. Yu. Zhitkovskii, Sov. Phys.—Acoust. (USA) **26**, 363 (1980).
5. N. C. Makris, L. Z. Avelino, and R. Menis, J. Acoust. Soc. Am. **97**, 3547 (1995).
6. N. C. Makris, S. Jagannothan, and A. Ignisca, Oceanography **23**, 204 (2010).
7. Ch. Holland, J. Acoust. Soc. Am. **119**, 1373 (2006).
8. D. E. Weston and P. D. Hocking, J. Acoust. Soc. Am. **87**, 639 (1990).
9. K. LePage, J. Acoust. Soc. Am. **106**, 3240 (1999).
10. V. A. Grigor'ev, V. M. Kuz'kin, and V. G. Petnikov, Acoust. Phys. **50**, 37 (2004).
11. R. Goldhahn, G. Hickman, and J. Krolik, J. Acoust. Soc. Am. **124**, 2841 (2008).
12. F. H. Li, Y. J. Zhang, R. H. Zhang, and J. J. Liu, Science Chin. Phys. Mechan. Astron. **53**, 1408 (2010).
13. S. D. Chuprov, in *Acoustics of Ocean* Ed. by L. M. Brekhovskikh and I. B. Andreeva, (Nauka, Moscow, 1982) [in Russian].
14. V. M. Kuz'kin, I.-T. Lin, A. A. Lun'kov, J. F. Linch, and V. G. Petnikov, Acoust. Phys. **57**, 381 (2011).
15. V. A. Gordienko, *Vector–Phase Methods in Acoustics* (Fizmatlit, Moscow, 2007) [in Russian].
16. W. M. Carey, J. Acoust. Soc. Am. **104**, 831 (1998).
17. T. F. Duda, J. M. Collis, Y.-T. Lin, A. E. Newhall, J. F. Lynch, and H. A. de Ferrari, J. Acoust. Soc. Am. **131**, 1782 (2012).
18. J. Max, J.-C. Carre, and F. Peltje, *Methodes et techniques de traitement du signal et applications aux mesures physiques. Tome 1. Principes generaux et methodes classiques*, (1981; Mir, Moscow, 1983).
19. W. J. Pearson, G. Neumann, and R. W. James, *Practical Method for Observing and Forecasting Ocean Waves by Means of Wave Spectra and Statistics,* (US Navy Hydr., 1955), vol. 284.
20. D. Rouseff, Waves Random Media **11**, 377 (2001).
21. G. L. Spain and W. A. Kuperman, J. Acoust. Soc. Am. **106**, 2454 (1999).
22. L. A. Brooks, M. R. F. Kidner, A. C. Zander, C. H. Hansen, and Z. Y. Zhang, Techniques for extraction of the waveguide invariant from interference patterns in spectrograms, *Proc. Acoustics, Christchurch, New Zealand, 2006.*
23. V. M. Kuz'kin, M. V. Kutsov, and S. A. Pereselkov, Acoust. Phys. **59**, 686 (2013).
24. V. M. Kuz'kin, M. V. Kutsov, and S. A. Pereselkov, Acoust. Phys. **60**, 405 (2014).

Translated by A. Carpenter